ELSEVIER

Biochimica et Biophysica Acta 1458 (2000) 28–42

BIOCHIMICA ET BIOPHYSICA ACTA
BBA

www.elsevier.com/locate/bba

Review

Calculation of isotope effects from first principles

Steve Scheiner *

Department of Chemistry, Southern Illinois University, Carbondale, IL 62901-4409, USA

Received 1 November 1999; accepted 1 December 1999

Abstract

Various means of calculating the effect of changing the mass of a given atom upon a chemical process are reviewed. Of particular interest is the deuterium isotope effect comparing the normal protium nucleus with its heavier deuterium congener. The replacement of the bridging protium in a neutral hydrogen bond such as the water dimer by a deuterium strengthens the interaction by a small amount via effects upon the vibrational energy. In an ionic H-bond such as the protonated water dimer, on the other hand, the reverse trend is observed in that replacement of the bridging protium by dimer weakens the interaction. In addition to the stability of a given complex, the rate at which a proton transfers from one group to another is likewise affected by deuterium substitution, viz. kinetic isotope effects (KIEs). The KIE is enlarged as the temperature drops, particularly so if the calculation of KIE includes proton tunneling. The KIE is also sensitive to any angular distortions or stretches present in the H-bond of interest. KIEs can be computed either by the standard transition state theory which is derived via only two points on the potential energy surface, or by more complete formalisms which take account of larger swaths of the surface. While more time intensive, the latter can also be applied to provide insights important in interpretation of experimental data.

Keywords: Transition state theory; Hydrogen bond; Proton transfer; Tunneling; Reaction path; Molecular dynamics

1. Introduction

The fact that atoms come in more than one weight has opened a window for researchers into the mechanisms of various chemical and biological processes. Because they are chemically indistinguishable, the various isotopes of a given atom obey the same chemical principles: intrinsic bond strengths are the same, as are the energies needed to stretch and otherwise distort these bonds. On the other hand, their different masses cause these isotopes to behave differently in a dynamic sense, in much the same way that heavier objects tend to move more slowly than lighter ones. Kinetic isotope effects (KIEs), which refer to the differences in dynamic behavior between these isotopes, can be measured experimentally and provide detailed information about the mechanism of the reaction under investigation [1–3].

In its simplest manifestation, the manner in which a heavier mass affects a chemical reaction has to do with nuclear vibrations. Even in its ground state, an oscillator retains a certain amount of vibrational energy, commonly referred to as zero-point vibrational energy (ZPVE). This quantity is sensitive to the mass of the oscillator such that a lesser amount of ZPVE will be associated with a heavier atom. This difference in ZPVE affects the energy needed to climb to the top of the barrier, and thus the rate of the reac-

* Fax: +1-618-453-6408;
E-mail: scheiner@chem.siu.edu

0005-2728/00/$ – see front matter
PII: S0005-2728(00)00058-X

tion. Since the energy difference is directly related to the ratio of masses of the two pertinent isotopes, and since the ratio is much greater for D/H than for any other pair of isotopes, deuterium isotope effects will in general be much larger and hence more accurately measurable than will be the case for say, ^{18}O vs. ^{16}O. It is for this reason that the majority of isotope effects that have been studied compare the various isotopes of hydrogen.

Unfortunately, the origin of isotope effects is not quite so simple. In the first place, there are other factors that play a role, such as the partial occupation of excited vibrational states at physiological temperatures. Another important point is that the reaction coordinate is seldom so simple as to involve the motion of only one atom. In other words, the substituted isotope is not the only nucleus whose mass contributes to the observed isotope effect. In an extreme case, it is possible that the rate-determining step of a proton transfer reaction may consist primarily of the approach of the two heavy atoms, i.e. the shortening of the hydrogen bond, so that the mass of the transferring hydron is of little importance to the reaction rate.

The mass of a hydrogen (or deuterium) is small enough that it is not necessary for the particle to climb over the barrier. Instead, the nucleus may pass from reactants to products, remaining below the top of the barrier, in a process known as quantum mechanical tunneling. The rate of tunneling is very sensitive to the mass of the particle, but in a different way than the classical rate of climbing over the barrier. A great deal of work over the years, some of it described below, has led to acceptance of the fact that any quantitative understanding of deuterium isotope effects must include a reasonable treatment of tunneling.

This review attempts to provide an overview of various theoretical means of calculating isotope effects from first principles. After a brief introduction of the basic theory, Section 2 describes how the substitution of a protium by a deuterium can affect the energetics of formation, the strength, of a hydrogen bond. It discusses not only the normal H-bonds between neutral molecules, but also ionic variants where one of the two partners bears an overall electrical charge. Section 3 includes a discussion of a means of computing isotope effects upon the rate of proton transfer. It begins with perhaps the simplest treatment, transition state theory (TST), which focuses on two particular nuclear configurations, located at the bottom of the well and the top of the barrier. Section 4 takes the derivation a step further by considering the entire reaction path between reactants and transition state. A different approach entirely is outlined in Section 5. All the atoms are placed in a certain configuration approximating the reactants. They are then each allowed to take small steps along vectors that parallel the forces acting upon them. By repeating this process, a trajectory is generated in this molecular dynamics approach which is capable of treating isotope effects as are the methods described in the preceding sections.

2. Hydrogen bond strength

A starting point for our understanding of isotope effects approximates the potential energy for the stretching of a bond, V, as a simple harmonic function

$$V = 1/2k(r-r_o)^2 \quad (1)$$

where r represents the length of the bond and r_o its equilibrium value; k is a force constant related to the 'stiffness' of the bond. A simple quantum treatment of this problem [4] leads to the well known solution that the energy of the system depends upon a quantum number v

$$E_v = \left(v + \frac{1}{2}\right)\frac{h}{2\pi}\sqrt{\frac{k}{\mu}} \quad (2)$$

where h refers to Planck's constant and μ is the reduced mass corresponding to the atoms involved in the bond stretching motion. In the case where the bond stretch involves the motion of a hydrogen atom, μ is commonly approximated simply by the mass of the H. In most cases of biological interest, the system is in its ground vibrational state, so $v=0$. But it is important to note that E_v does not equal zero when $v=0$. Thus, each bond stretch has associated with it a residual amount of vibrational energy, even at 0 K, called the ZPVE. It is this ZPVE which is at the heart of isotope effects.

Since replacement of any atom such as hydrogen

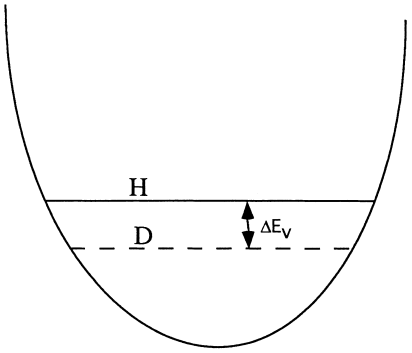

Fig. 1. ZPVEs associated with H and D nuclei.

by an isotope does not affect the electronic structure, k is independent of isotopic substitution. Because the mass appears in the denominator of Eq. 2, the heavier isotope has associated with it a lesser amount of ZPVE. This relationship is illustrated in Fig. 1 where the ZPVE of bonds involving the H and D atoms is indicated by the height of the vibrational energy level within the parabola that represents the potential energy for bond stretching, Eq. 1.

The above description refers to a diatomic molecule containing only one bond whereas most molecules of interest contain many atoms and bonds. An analysis of the multitude of forces between the N atoms leads to a recombination of the various bond stretches and bends into 3N-6 normal modes. Each such mode is independent of the others, with its own characteristic force constant k and reduced mass μ. Moreover, each normal mode reflects the symmetry of the entire molecule. In the case of water, for example, the three normal modes are illustrated in Fig. 2 where the two O–H stretches are recombined into a symmetric stretch where both bonds elongate simultaneously, and an antisymmetric stretch where one elongates as the other contracts. The third mode is a bend wherein the θ(HOH) angle alternately becomes larger and then smaller than its equilibrium value. Each of these three normal modes behaves as described above, and each contains a certain amount of ZPVE. In the case of HOH, an ab initio computation provides an estimate of 14.16 kcal/mol for the total ZPVE of these three modes [5].

Since each of the three modes involves the motion of a H atom, replacement by the heavier deuterium will reduce the ZPVE of each to a certain extent. In sum, the total ZPVE, summed over all three modes, of HOH suffers a decline of approximately 2 kcal/mol for each H→D replacement. The ZPVE calculated for HOD is 12.25 kcal/mol; doubly deuterated DOD has a ZPVE of 10.31 kcal/mol [5].

One of the important questions of biological systems concerns how the strength of a hydrogen bond is affected by deuteration. Before answering this question, it must first be understood that the H-bond energy refers to the stabilization that arises when a pair of molecules like AH and B come together to form the interaction. In other words, the H-bond energy can be defined as the difference in energy between the two separated monomers, and the resulting complex:

$$\begin{aligned} &\mathrm{AH} + \mathrm{B} \rightarrow \mathrm{AH}\cdots\mathrm{B} \\ &E_{\mathrm{HB}} = E(\mathrm{AH}\cdots\mathrm{B}) - [E(\mathrm{AH}) + E(\mathrm{B})] \end{aligned} \tag{3}$$

If one of the two molecules, say AH, is deuterated, of course the ZPVE of this molecule is reduced. But this reduction occurs in AH not only when it is isolated, but also when it occurs as part of the AH···B complex. The issue then becomes a matter of learning whether the ZPVE is reduced more in the former or in the latter. In fact, the question is somewhat more complicated. Once the complex has been formed, the vibrational modes of the two subunits 'mix' to some extent. Hence, replacement of a H atom by D in the AH part of the system affects not only AH modes, but also those within the partner B subunit. Moreover, the formation of the com-

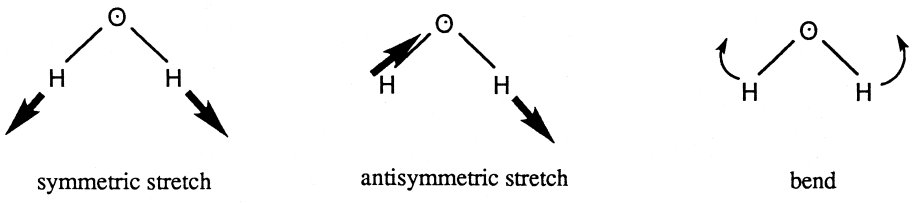

Fig. 2. Normal vibrational modes of H_2O molecule.

plex leads to the presence of several new vibrational modes, modes that were not present in either of the isolated monomers. These intermolecular modes generally reflect the motions of one entire subunit relative to the other, and can also be influenced by the replacement of a H atom by a heavier D nucleus.

2.1. Neutral H-bonds

The above points can best be illustrated by a concrete example, for which we take the water dimer as a model system. One can rewrite Eq. 3 for this case, emphasizing that one molecule will be the proton donor in the dimer, and the other the acceptor.

$$\begin{aligned} &HOH + OH_2 \rightarrow HOH\cdots OH_2 \\ &E_{HB} = E(HOH\cdots OH_2) - [E(HOH) + E(OH_2)] \end{aligned} \quad (4)$$

As pointed out above, the total ZPVE of a single water molecule has been calculated to be 14.16 kcal/mol. Hence, the total of a pair of these isolated molecules, the last term in Eq. 4, is 28.32 kcal/mol. A computation of the water dimer complex shows that the six combined intramolecular modes, three in each monomer, add up to 27.30 kcal/mol. The three intermolecular modes, absent in the monomers, sum to 2.44 kcal/mol. The combination yields a total of 29.74 kcal/mol, 1.42 kcal/mol more than the sum of the isolated monomers. This rise in ZPVE in the complex, compared to the sum of monomers, represents a bite out of the H-bond energy. That is, the electronic contribution to the H-bond energy is 6.80 kcal/mol, which is reduced by 1.42 kcal/mol to an effective binding energy of 5.38 kcal/mol.

Let us now consider the situation when one of the hydrogen atoms is replaced by D. In particular, we choose the bridging atom of the complex. Whereas the ZPVE of the unsubstituted OH_2 molecule remains at 14.16 kcal/mol, that of its HOD partner is reduced to 12.25 kcal/mol, for a total of 26.41 kcal/mol. The deuterosubstitution in the $HOD\cdots OH_2$ complex affects all the modes, yielding a total ZPVE of 27.60 kcal/mol. The latter quantity is greater than the monomer sum by 1.19 kcal/mol. Note that this difference is less than the corresponding value of 1.42 kcal/mol for the unsubstituted system. As a result, when 1.19 is subtracted from the electronic contribution of 6.80 kcal/mol, the resulting H-bond energy in $HOD\cdots OH_2$ is greater than that in $HOH\cdots OH_2$. In summary, then, the replacement of the bridging hydrogen by a deuterium has strengthened the H-bond by 0.23 kcal/mol.

Suppose, however, that the H chosen for replacement is not the bridging atom, but is instead one of the peripheral atoms, e.g. $DOH\cdots OH_2$ or $HOH\cdots OHD$. Calculations reveal [5] that such a substitution lowers the ZPVE of the complex, and of the monomer pair, by very nearly equal amounts. Consequently, this peripheral deuterosubstitution has no net effect upon the H-bond energy. It is hence concluded that replacement of hydrogen by deuterium will strengthen the H-bond, by some 0.2 kcal/mol, but only if it is the bridging hydrogen that is replaced. These computational findings are in consonance with spectroscopic measurements in Kr matrix [6].

The previous analysis refers specifically to the water dimer, with a single H-bond connecting a pair of molecules. However, most of the water molecules that occur in biological systems, or in aqueous solution, are involved in several H-bonds at once, in both a donor and acceptor role simultaneously. Calculations of the water trimer, where each molecule is so engaged as both donor and acceptor [5], indicate that the trends observed for the dimer emerge unchanged in larger aggregates: replacement of each bridging hydrogen by a deuterium nucleus strengthens the corresponding H-bond by some 0.2 kcal/mol.

Of course, water is not the only molecule that involves itself in hydrogen bonds, nor is its hydroxyl the only group that forms such bonds. Calculations of the type described above were extended to a range of chemical groups that are commonly involved in H-bonds [7]. The H-bond formed by a carboxyl group was found to be strengthened by 0.10 kcal/mol when the protium is replaced by deuterium. The increase is slightly larger, 0.13–0.16 kcal/mol, when the H/D exchange takes place at the NH of an amide group. In summary, it appears that most H-bonds are strengthened when the bridging hydrogen is replaced by deuterium. The amount is somewhat variable, but calculations estimate this strengthening to lie in the 0.1–0.2 kcal/mol range.

2.2. Ionic H-bonds

The above discussion has been concerned with the normal sorts of H-bonds that occur between pairs of neutral molecules. However, when one of the partners bears an electrical charge, the interaction is usually much stronger. For example, whereas the binding energy of a pair of neutral water molecules is 4–5 kcal/mol in the gas phase, the interaction of a neutral water with either a $(H_3O)^+$ or OH^- ion is on the order of 25–30 kcal/mol. These much stronger ionic H-bonds often differ from their neutral counterparts in a second important respect. In the neutral water dimer, there is no question but that the bridging hydrogen retains its covalent association with the proton donor molecule in $HOH\cdots OH_2$. While the covalent O–H bond might be stretched a small amount, less than 0.01 Å, it remains intact and is much stronger than the intermolecular H···O contact. The situation in an ionic system such as $H_2OH^+\cdots OH_2$ is quite different. The potential for motion of the bridging hydrogen becomes much flatter, allowing the proton to stretch far away from the donor oxygen atom. In some cases, the minimum in this potential shifts all the way to the center of the O···O bond, yielding a symmetric single-well potential. Even when this does not occur, the barrier separating the $H_2OH^+\cdots OH_2$ from the $H_2O\cdots{}^+HOH_2$ minima is commonly quite small.

Regardless of whether the potential is formally of single- or double-well type, the important fact is that the proton transfer potential in the ionic system is distinctly different than in the weaker H-bond connecting a pair of neutral molecules. It is this difference that leads to a reversal in the trends noted above for normal H-bonds. Whereas the latter is strengthened when the bridging H is replaced by D, the opposite occurs in a ionic system. The $H_2OD^+\cdots OH_2$ system is hence bound 0.4 kcal/mol more weakly than is $H_2OH^+\cdots OH_2$ [5].

This perhaps surprising behavior can be understood in terms of the very flat potential for proton motion along the H-bond. The force constant k (see Eq. 1) is fairly small in this case, leading to a low ZPVE, as illustrated on the right side of Fig. 3. As a result, there is not much difference in ZPVE between the case when the nucleus has a mass of 1 or 2, and the vibrational energy is lowered by only a little

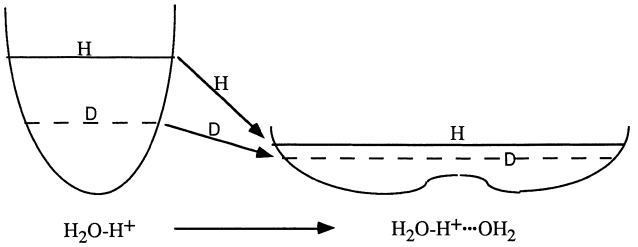

Fig. 3. Zero-point vibrational levels for H and D in the case of an isolated species, on the left, and an ionic H-bond on the right.

when H is replaced by D. This situation contrasts with the case of the isolated monomers, prior to formation of the H-bond, on the left side of Fig. 3. The force constant for OH stretching in the $(H_3O)^+$ unit is large, causing a much greater loss of vibrational energy if H is replaced by the heavier D. As illustrated in Fig. 3, then, both the H and D situations drop in vibrational energy, i.e. are stabilized, by formation of the H-bond. However, this stabilization is considerably smaller for the deuterium case, making the D-bond weaker than the H-bond. This same reasoning applies also to the anionic analogue $(HOH\cdots OH)^-$, although the bond weakening caused by the deuterosubstitution is estimated to be smaller here, only about 0.1 kcal/mol [5].

The above concepts are not limited to the specific systems above, which were presented primarily for illustrative purposes. For example, the preference of the mixed (HF,HD) system to adopt the FD···FH geometry over FH···FD has been understood for some years [8,9], as has the analogous ClD···ClH system [10]. Other systems for which there is experimental evidence of the preference of a D-bond over a H-bond include combinations of water with ammonia [11,12], formaldehyde and formamide [13], and olevines [14]. The reversal in this trend that occurs in ionic systems, i.e. the preference for a bridging protium over deuterium, has also been confirmed by other groups [15–18].

3. Proton transfer rates

3.1. TST

The simplest and perhaps most common means of estimating reaction rates is based on Eyring's TST

wherein reactants proceed to products over an energy barrier of height $E^{\ddagger}$ [19–21]. At the top of the barrier lies a configuration of atoms known as the transition state, or activated complex, which is characterized as a first-order stationary point on the potential energy surface (PES). In other words, this configuration is a minimum with respect to all nuclear motions except one, the reaction coordinate which takes reactants to products. Included then among its vibrational frequencies is one which is mathematically imaginary since it corresponds to a maximum rather than a minimum along this coordinate. The reaction rate can be calculated as a function of the temperature T:

$$k_{TST}(T) = (2.084\times10^{10}\ s^{-1}\ K^{-1})\kappa(T)(Q^{\ddagger}/Q)T \exp(-E^{\ddagger}/RT) \quad (5)$$

Q refers to the total partition function of the reactants, including translational, vibrational and rotational degrees of freedom. $Q^{\ddagger}$ has the corresponding meaning for the transition state, except that the imaginary vibrational frequency is of course excluded. Since the process of interest here is proton transfer, and because this particle is so light, it is generally considered a poor approximation if no account is made for tunneling, i.e. the rate ought to have some contribution from the transition of reactants to products even where there is insufficient energy to surmount the classical energy barrier. The curvature at the maximum makes its appearance within the quantity $\kappa(T)$ which allows for this tunneling. Perhaps the simplest and most common form of this expression is attributed to Wigner [22].

$$\kappa(T) = 1 + [h\nu_i/RT]^2/24 \quad (6)$$

wherein ν_i refers to the imaginary frequency and h is Planck's constant.

Replacing the bridging proton by a deuteron will affect the various quantities in Eq. 5 differently. The effect of deuterosubstitution on the rate is known as the KIE and can be expressed [23] as follows.

$$KIE = k_H/k_D = \kappa_H/\kappa_D \times MMI \times EXC \times ZPE \quad (7)$$

κ again refers to a tunneling correction, which may take the form of Eq. 6, in which case the tunneling contribution to the KIE will arise through the effect of deuterosubstitution upon the imaginary frequency ν_i. The MMI term encompasses the mass and moment of inertia, which originate in the translational and rotational partition functions. The effects of the isotopic replacement upon the ZPVE are focused in the ZPE term, whereas the effects of population of vibrational states above the ground state are associated with EXC.

The foregoing formulation is termed a canonical treatment as it includes an averaging over the range of different energies. One can evaluate microcanonical rate constants, each one pertinent to a particular energy, in various ways, perhaps the most popular of which has been given the RRKM acronym of four of its developers [24–26]. When the energy of the system lies below the transfer barrier, the RRKM formalism would normally predict no reaction at all. In order to allow for tunneling to occur in such a case, one can compute a transmission coefficient through the barrier at each energy and include this tunneling term in the rate expression [27]. These microcanonical rates can then be summed over the full range of energies, incorporating the density of states and a Boltzmann term, to arrive at an RRKM equivalent of Eq. 5. One advantage of this treatment over canonical TST is the ability to evaluate the tunneling contribution separately for each energy, rather than a blanket expression such as Eq. 6.

3.1.1. Bent H-bonds

As it is well known that hydrogen bonds in proteins are seldom linear, proton transfers must often occur across angularly distorted H-bonds. Computational evidence has mounted over the years that increasing angular distortion leads to a progressively higher energy barrier to the proton transfer [28–30]. Calculations were carried out to ascertain how these angular deformations might affect the isotope effects of the proton transfer occurring within them. In order to model this situation, a trio of related $H_2N(CH_2)_nNH_3^+$ systems were considered [31]. As illustrated in Fig. 4, the $n=1$, 2 and 3 systems differ quite drastically in the characteristics of the intramolecular NH···N hydrogen bond. These properties are reported in Table 1 where it may be seen that the H-bond is much longer for $n=2$ and 3 than for $n=1$.

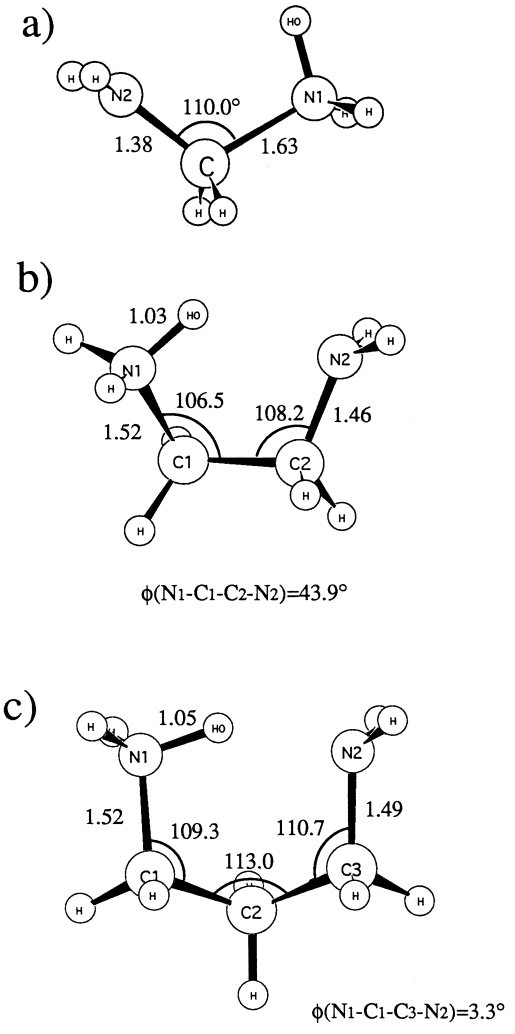

Fig. 4. Geometries of $H_2N(CH_2)_nNH_3^+$ systems. Details of intramolecular H-bonds are reported in Table 1.

More importantly, the latter system is grossly distorted from the optimal linear situation which would have $\theta(NH\cdots N)=180°$; the H-bonds are also bent for $n=2$ and 3 but not by as much. The last row of Table 1 makes it clear that the highly distorted H-bond for $n=1$ has much the highest proton transfer barrier, even though this is the shortest H-bond of the three.

The KIEs of these three systems were evaluated via Eqs. 5–7 and are illustrated as a function of the reciprocal temperature as the solid curves in Fig. 5. The two curves representing $n=1$ and 2 are approximately parallel in the temperature range under consideration. For the high temperatures exceeding 1000 K on the left side of the figure, the KIE approaches unity asymptotically as one might expect. As the temperature drops, the KIE climbs, approaching a value of 10 as T reaches 250 K. It should be noted that the more strained H-bond, with its higher transfer barrier, manifests a higher value of the KIE, but not drastically so.

An alternate means of computing transfer rates, and thence KIE, arises from the microcanonical treatment. A primary difference with the canonical calculations above is the ability to vary the tunneling contribution at each energy below the barrier. This tunneling was calculated by fitting an Eckart potential to the transfer potential and computing the tunneling transmission coefficient by an analytical expression [27,31]. When averaged to provide canonical rate constants, the KIEs of each system are illustrated by the broken curves in Fig. 5. A principal difference with the TST data is the much greater temperature sensitivity of these broken curves. A second prime distinction is the much larger discrepancy between the $n=1$ and $n=2$ cases, i.e. the microcanonical treatment of tunneling makes the KIE much more sensitive to the geometric aspects of the H-bond. Note that in this framework, the KIE can reach much larger values, as high as 10^4 for $T=250$ K for the highly strained $n=1$ system.

The framework of Eq. 7 permits one to draw inferences about the fundamental origin of the observed KIE. While the Wigner tunneling contribution (κ_H/κ_D) does show the same general behavior of an inverse relationship with T, this term is rather small, never climbing above two, even at low temperatures. Rather, it is the zero-point energy that is the dominant factor in the climb of KIE with diminishing temperature. This observation can simply be understood since the rate in Eq. 5 depends exponentially upon the transfer barrier $E^‡$. The heavier D nucleus lowers the ZPVE of the equilibrium geometry of the

Table 1
Geometric and energetic aspects of the intramolecular H-bond in $H_2N(CH_2)_nNH_3^+$

	$n=1$	$n=2$	$n=3$
R(N··N) (Å)	2.44	2.64	2.69
θ(NH··N) (°)	81	125	149
r(NH) (Å)	1.009	1.030	1.053
$E^‡$ (kcal/mol)	29.7	4.2	0.8

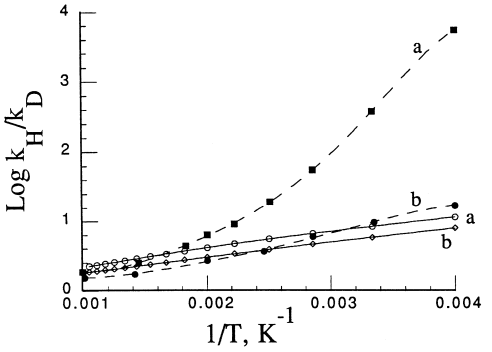

Fig. 5. KIEs of $H_2N(CH_2)_nNH_3^+$ systems for (a) $n=1$ and (b) $n=2$. Solid curves were computed by TST theory, with a Wigner correction for tunneling. Broken curves correspond to computation by microcanonical scheme (see text).

reactants (see Fig. 1), leaving a higher climb to the top of the barrier, and hence a larger $E^{\ddagger}$. As the temperature drops, this distinction in $E^{\ddagger}$ takes on added mathematical impact in the $\exp(-E^{\ddagger}/RT)$ term of Eq. 5.

However, this conclusion must be placed within the perspective of the microcanonical findings. Comparison of the solid and broken curves of Fig. 5 indicates that the Wigner correction severely underestimates the contribution of tunneling to the KIE. It is only in this context that ZPE plays a dominant role. When tunneling is more accurately included, however, its importance to the KIE becomes readily apparent [32]. Theoretical treatments of KIEs would therefore seem to be heavily dependent on a realistic treatment of tunneling.

3.1.2. *Effect of barrier height*

One can further probe the question of the influence of the height of the energy barrier to proton transfer upon the magnitude of the KIE. A microcanonical treatment permits a dissection of the rate of the reaction into contributions from any given energy level. This sort of data are illustrated in Fig. 6 for a prototype system wherein a proton is being transferred between C atoms in a model system $(H_3C{\cdot}H{\cdot\cdot}CH_3)^-$. The rates were calculated using RRKM theory, and include a tunneling contribution for energies lying below the top of the transfer barrier [33]. Three different possibilities were considered as transfer barriers, ranging between 12.1 and 23.2 kcal/mol, as indicated in the figure. For each value of the energy barrier, the rate was computed for both $(H_3C{\cdot}H{\cdot\cdot}CH_3)^-$ and its perdeuterated analog $(D_3C{\cdot}D{\cdot\cdot}DH_3)^-$.

These rates are presented as a function of energy in Fig. 6 where the solid and broken curves refer respectively to the protio and deutero situations. Taking the undeuterated $(H_3C{\cdot}H{\cdot\cdot}CH_3)^-$ system, with barrier 23.2 kcal/mol, as an example, the rate is very small when the energy level E is below this value since the transfer must take place via tunneling. One may note from the figure how precipitously this tunneling rate drops as the energy level sinks further and further below the top of the barrier at 23.2 kcal/mol. If one is above this barrier, i.e. for $E>23.2$, transfer can take place via the classical process, so the rate climbs more slowly as the temperature increases, asymptotically approaching its infinite temperature limit at the far right of the figure. In the more general case with no particular barrier specified, the rate constant spans many orders of magnitude lying in the approximate range of 10^6–10^8 s^{-1} at high energy but dropping below 10^{-8} s^{-1} as the energy drops. It is also apparent that the rate is quite sensitive to activation energy, as higher values of $E^{\ddagger}$ are associated with much lower rates.

Note that in each case, and for any energy considered, the system containing the lighter isotope has a higher rate constant k. The discrepancy between the H and D systems is fairly small at high energies but becomes more pronounced as the energy diminishes.

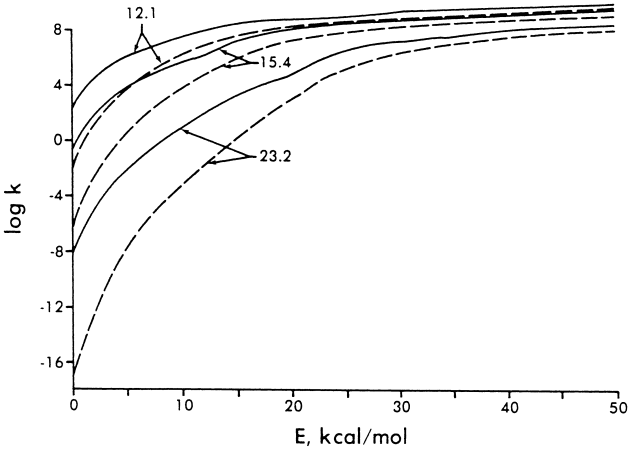

Fig. 6. Microcanonical rate constants (s^{-1}) computed for $(H_3C{\cdot}H{\cdot\cdot}CH_3)^-$ (solid curves) and its perdeuterated analog $(D_3C{\cdot}D{\cdot\cdot}DH_3)^-$ (dashed curves) [33]. Numerical label on each curve represents the height of the energy barrier to proton transfer that is used to compute the rate constant.

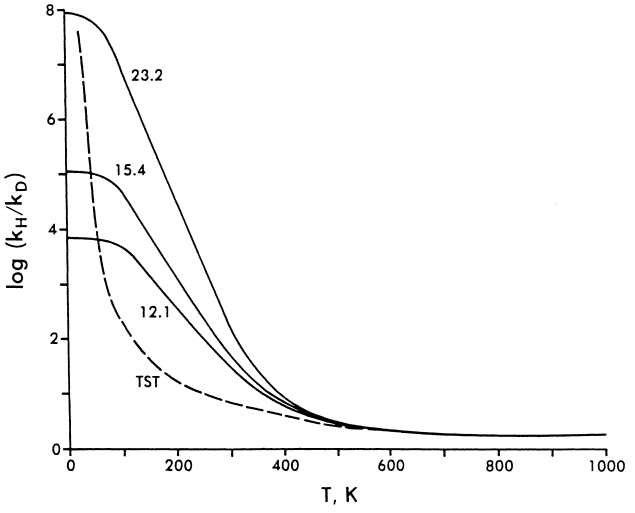

Fig. 7. KIEs for $(H_3C{\cdot}H{\cdot\cdot}CH_3)^-$ as a function of temperature for three different assumed values of the energy barrier. The dashed curve corresponds to k_H/k_D that would be calculated by simple TST, with no provision for tunneling.

The ratio between these two isotopic variants is illustrated as a function of temperature in Fig. 7. Also included as the dashed curve for illustrative purposes is the isotope effect as computed by simple TST, with no provision for tunneling. When the temperature exceeds about 500 K, there is little discrepancy between the TST and other values; nor is the energy barrier significant. The high-temperature asymptote of k_H/k_D is 1.12. As the temperature declines below 500 K, most of the curves begin to rise rather steeply. This temperature sensitivity is particularly large for the higher transfer barriers. The KIE is predicted to be capable of reaching very large values, in excess of 10^4. It is quite interesting to observe that as the temperature drops into the 50–100 K range, the sharp increase of k_H/k_D with diminishing T levels off. A number of features of the solid curves in Fig. 7 are consistent with various experimental observations that reproduce the level behavior at low T, the steep sensitivity to T in higher temperature ranges, and the very high values that k_H/k_D can attain at low T [34–41].

As mentioned above, the broken curve in Fig. 7 indicates the KIE that is computed for this same system using conventional TST. This variant of the canonical approach does not include a contribution from tunneling. Note that at high temperatures, exceeding about 500 K, TST yields a KIE quite equivalent to the microcanonical treatments which include tunneling. It is only at lower temperatures that the various approaches diverge. For most temperatures, the TST isotope effect is considerably lower than the microcanonical estimates, suggesting the importance of tunneling. It is particularly interesting, however, to note that as the temperature drops further, below 100 K, the TST prediction of k_H/k_D begins to climb dramatically, and does not level off as do the microcanonical treatments with tunneling included.

3.1.3. Related systems

A similar sort of transition state approach has been taken more recently for a series of hydrogen transfer reactions, all involving the amino radical NH_2 [42]. The rates of the reactions were computed using the standard TST approach with a Wigner tunneling correction. The abstraction of a hydrogen from H_2 to form NH_3 has been studied experimentally [43–45], as has the reaction with D_2, which provides a source of comparison. The theoretical rates were found to be smaller than the experimental values for temperatures less than about 1000 K, using quantum chemical data. This underestimate is not surprising since the Wigner correction underestimates tunneling contributions. Much better agreement was found if the barrier was treated as an adjustable parameter, and was lowered by 1 or 2 kcal/mol. The deuterium isotope effect for the NH_2+D_2 reaction, relative to NH_2+H_2, was computed to be 2.6 at 740 K and 2.0 at 1140 K, less than experimental measurements of 3.3 and 2.4 at the same two temperatures [42].

The reaction of NH_2 with CH_4 also has a solid base of experimental data [43,46,47]. The computed rate constants fell generally within the error bars of the various experimental rate constants, although it was difficult to obtain uniformly good descriptions over the entire temperature range [42]. Deuterium isotope effects for this same reaction with CD_4 were found to vary between 1.6 at 2000 K and 25.4 at 300 K. An inverse KIE, i.e. a faster reaction rate, is obtained when it is the hydrogen acceptor NH_2 which is deuterated; this secondary isotope effect is between 1.1 and 1.9.

In the case of the symmetric reaction involving hydrogen exchange between NH_3 and NH_2, the authors attempted to compute the isotope effect in-

volved in ^{15}N substitution [42]. The resulting KIE was very small, with the reaction being slowed down by only 1–2% by the heavier nucleus. Primary and secondary deuterium isotope effects, monitoring ND_3+NH_2 and NH_3+ND_2, were found to be quite similar in magnitude to the results for NH_2 with CH_4. Isotope effects of a similar magnitude were obtained as well for the reaction between NH_2 and H_2O [42].

3.1.4. Larger model systems

A similar formalism may be applied to much larger systems that more closely approximate biological situations. For example, enzymatic catalysis by alcohol dehydrogenase shows isotope effects that can be successfully modeled. Rucker and Klinman [48] applied the Bigeleisen notions [23,49] to the reaction of models of benzyl alcohol with NAD^+, the enzyme cofactor. Rather than calculate the vibrational frequencies by quantum chemistry, an empirical force field was employed. (This sort of approach can be rather tenuous, particularly in attempts to estimate force constants for a transition state [50]). Tunneling was incorporated by a correction due to Bell [2], which considers the barrier to have an inverted parabolic shape, and is a function of the curvature of the barrier along the reaction coordinate, as well as the temperature. A number of different parameter sets were explored for their ability to reproduce experimental isotope effects, including a model similar to that used earlier [51]. Some of the data were quite good, mimicking experimental quantities rather closely. The authors concluded that tunneling is rather important, and can make the major contribution to the secondary KIE. This result confirms other work by the same group [52–54].

There are other treatments which attempt to incorporate a more complete model in computing isotope effects [55]. The importance of tunneling has also become evident in the enzymatic cleavage of a C–H bond by the enzyme methylamine dehydrogenase [56]. The large KIE of 17, and its independence upon temperature, coupled with a temperature sensitivity of the reaction rate, led the researchers to propose that the tunneling is driven by vibrational motions occurring within the entire protein. The results led to questions about the suitability of TST to investigate systems of this type, even with some incorporation of tunneling effects. The authors suggest that the classical reaction path followed by TST is not necessarily the proper route, and that the reaction might in fact avoid climbing a static barrier [57].

4. PES

The rate of a chemical reaction depends upon the entire multidimensional PES that spans all of the various nuclear motions. Conventional TST is hence quite limited in the sense that information about the reaction rate is derived exclusively from only two points on the entire PES. In the case of proton transfer reactions, the two pertinent nuclear configurations are the equilibrium geometry of the AH···B complex and the transition state, with the proton approximately midway between the donor and acceptor groups. One means of obtaining a more complete assessment of a proton transfer reaction is by following the process along the reaction path from AH···B as a starting point, up the barrier to the transition state A··H··B, and then back down to product A···HB. One advantage of a 'direct dynamics' treatment such as this is that it samples a larger fraction of the PES, but it must be understood that this sampling is by no means complete, confining itself primarily to the reaction path.

The path is defined by first identifying the transition state for the process, the same transition state geometry as is employed in the TST formalism [58]. An intrinsic reaction coordinate (IRC) is elucidated [59,60] by following a minimum energy path, by a steepest descent approach, down to the reactant AH···B. At each point along this path, vibrational frequencies are computed for the geometry in question, and used to generate a vibrational partition function. Adding this vibrational energy to the pure electronic energy provides a ground state vibrationally adiabatic potential curve, with an effective barrier. The entire path can then be used to generate a unimolecular canonical variational TST rate constant [61,62]. Tunneling effects can be included in several ways. One approach involves a semiclassical adiabatic ground state approximation along the minimum energy path [63], and a Boltzmann average of semiclassical probabilities. A second allows for a

small degree of curvature which can cut corners from the reaction path [64].

4.1. Small model systems

An analysis of the minimum energy path for the transfer reaction in $(H_3C{\cdot}H{\cdot\cdot}CH_3)^-$ shows it to be composed of several steps or phases, nearly separate and distinct. In the initial phase of the reaction, the two CH_3^- groups begin to approach one another, shortening the H-bond distance R(C··C). Only after this bond has shortened does the bridging proton begin to move appreciably away from the donor C atom toward the center of the bond. Upon reaching the transition state $(H_3C{\cdot\cdot}H{\cdot\cdot}CH_3)^-$, the entire process reverses itself. The proton continues to move toward the acceptor carbon, followed then by a re-elongation of R(C··C), to eventually reach the product $(H_3C\cdots HCH_3)^-$.

The rate constants computed for this process are presented as an Arrhenius plot in Fig. 8 where CVT serves as a reference point to conventional TST, with no tunneling. It might be noted that this approach leads to a linear relationship between log k and the inverse of the temperature, the classical Arrhenius behavior. As predicted by the methods described above, tunneling becomes important for this reaction as the temperature drops below 500 K. To the right of this temperature in Fig. 8, the various schemes that include tunneling diverge markedly from the classical results, indicating that the process becomes progressively more dominated by tunneling. Taking 300 K as one example, the CVT/MEPSAG rate constant exceeds the non-tunneling CVT value by a factor of 11. This tunneling-induced magnification climbs to 250 at 200 K, and to as high as 10^8 at 100 K.

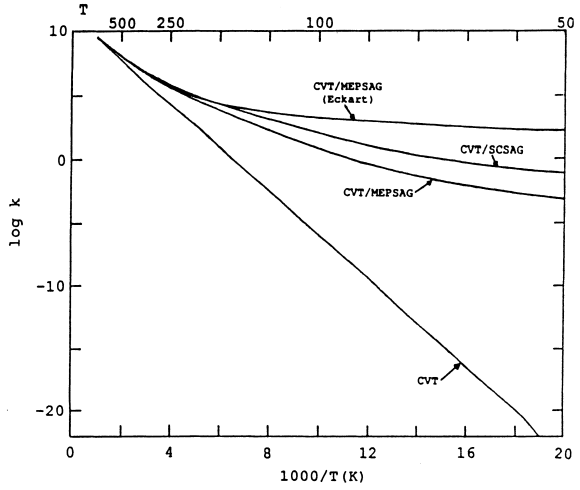

Fig. 8. Rate constants (s^{-1}) computed for proton transfer in $(H_3C{\cdot}H{\cdot\cdot}CH_3)^-$, plotted in an Arrhenius fashion. CVT refers to conventional transition state approach. MEPSAG corresponds to minimum energy path semiclassical ground state approximation to tunneling; the curvature-dominant small curvature tunneling approximation is represented by SCSAG.

The previous means of computing reaction rates lend themselves more readily to assessment of KIEs than the present procedure which requires one to follow the reaction path from reactants to transition state. Since the various parameters of the PES are scaled by atomic masses, computation of the rate constant for an isotopically substituted variant of $(H_3C{\cdot}H{\cdot\cdot}CH_3)^-$ requires more than a simple adjustment of several parameters. Rather, a new reaction path must be elucidated and followed for each particular isomer, along with the vibrational properties along this new path.

A more recent calculation on a related transfer process made use of a similar means of computing the reaction rate. Masgrau et al. [65] considered the transfer of a hydrogen from water to OH radical in (HOH···OH) using a variational TST formalism. Rather than following the IRC, the authors considered a so-called 'distinguished' reaction coordinate wherein one particular parameter, say a bond length, is arbitrarily chosen as reaction coordinate. This parameter is varied in uniform increments, and at each point, all other geometrical parameters are optimized, thereby tracing out the energy for this particular path. In the case of (HOH···OH), the distance between the bridging hydrogen and one of the O atoms was chosen as the reaction coordinate. Other than this choice of reaction path, which differs from the true minimum energy path, the rate constant calculation is very much like that discussed above. The same quantity was calculated for isotopically substituted variants by assuming no change in the reaction path, since the distinguished reaction path is in fact independent of the atomic masses.

The energy barrier for the transfer of the H between the two O atoms in this system was computed to be some 18–22 kcal/mol, depending upon the

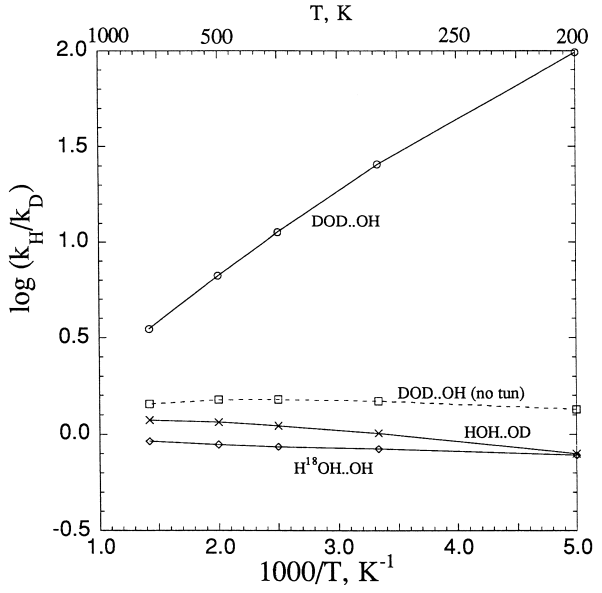

Fig. 9. KIEs computed for proton transfer in (HO·H··OH), plotted as a function of reciprocal temperature. Each curve is labeled with the particular isotopic substitution studied. The broken curve represents the KIE in the absence of tunneling. Rather than k_H/k_D, the property plotted for the ^{18}O-substituted system is k_{16}/k_{18}. Data taken from [65].

quantum chemical level of theory applied. The reaction rates were computed over a range of temperatures between 200 K and 700 K, varying from 10^{-15} at the higher temperature, down to 10^{-18} at 200 K. The deuterium isotope effects are illustrated as an Arrhenius plot of log (KIE) versus the reciprocal temperature in Fig. 9. For double deuterosubstitution in DOD··OH, log (k_H/k_D) varies approximately linearly with $1/T$, reaching a value of 100 at 200 K, as indicated by the upper curve in Fig. 9. This behavior contrasts sharply with the broken curve which represents the same quantity, but with tunneling neglected. The k_H/k_D ratio in this case is rather static, remaining in the neighborhood of 1.5 throughout the entire temperature range.

Also included in Fig. 9 are other patterns of isotopic substitution. Replacement of a peripheral H atom, i.e. one that is not bridging, yields so-called secondary KIEs of nearly unity. In fact, the KIE of the HOH··OD system diminishes as the temperature drops, at least in the range examined by the authors. This secondary KIE becomes less than one for low temperatures, indicative of a faster reaction for deuterium than for protium.

Most studies of isotope effects concern themselves with the distinction between H and D. A principal reason for this focus is that the masses of these two isotopes differ by a factor of two, quite a large ratio. In comparison, the mass ratio for oxygen, ^{18}O/^{16}O, is only 1.11. This smaller ratio is expected to lead to much smaller isotope effects, perhaps too small to measure accurately. Moreover, a heavy atom like O will typically not be strongly involved in the nuclear motion that produces the proton transfer. For these reasons, the KIE for replacement of the oxygen atom in a system like HOH··OH is expected to be rather small. Indeed, the lowest curve in Fig. 9 confirms this expectation. Quite interesting is the finding that log (k_{16}/k_{18}) is negative; in other words, the rate of the proton transfer reaction is slightly faster with the heavier oxygen nucleus, in place of ^{16}O. Such a result is commonly termed an inverse isotope effect.

4.2. Larger models

The variational TST formalism can be applied to larger systems, better models of a full enzyme/substrate. A recent paper provides such an example, the conversion of 2-phospho-D-glycerate to phosphoenolpyruvate by enolase [66]. In fact, these authors concerned themselves with the initial step of the enzymatic cycle, a proton transfer reaction, for which a k_H/k_D of 3.3 has been measured [67]. Due to the size of the system, the PES was computed using a mixed quantum mechanical/molecular mechanical approach whereby the heart of the system, deemed most relevant to the reaction at hand, is considered explicitly by a quantum mechanical calculation, and the remainder is treated by an empirical force field. In this case, the full system consists of the entire protein plus surrounding water molecules. The reactant and saddle point geometries were determined by a classical mechanical dynamics trajectory. The barrier height for the reaction was determined in this way to be 17.0 kcal/mol; the reaction is endoergic by 2.6 kcal/mol. A variational transition state computation followed, using a multidimensional tunneling approximation that accounts for small curvature of the path [68].

The KIEs (k_H/k_D) for replacement of the primary bridging hydrogen by deuterium were found to vary between 1.3 and 4.7 at 300 K, depending upon the

particular level of theory employed. The classical variant of TST leads to the lowest estimate, while the quantum versions provide values quite close to experiment, particularly when variational TST is used. The authors went beyond the experimental data and attempted to compute secondary KIE, replacing the H atoms that are not directly involved in the proton transfer, those covalently bonded to N, by deuterium. When quantum effects are neglected, no such secondary effects could be detected, i.e. the KIE is unity. Adding quantum effects leads to a KIE in the range of 0.89–0.96, depending upon whether variational or conventional TST is used. The authors continued by testing the rule of the geometric mean developed by Bigeleisen [69] which predicts the combination of primary and secondary KIE, and concluded this rule is not satisfactory in this case.

5. Molecular dynamics

A very different way to theoretically study a chemical reaction begins by placing all atoms in an initial configuration. The forces on the atoms are determined by some quantum mechanical method. Alternatively, an empirical force field can be used for the same purpose, evaluating the forces acting on each atom, at any given nuclear configuration. The atoms are then moved by some small increment along their corresponding force vectors, creating a new nuclear arrangement, and a new set of force vectors. By repeating these steps many times, a trajectory is traced out in multidimensional phase space, that may lead from reactants to products. By running a large number of trajectories and treating the results statistically, one is able to arrive at a valid estimate of reaction rate constant. Of course this molecular dynamics method is sensitive to the procedure used to assess the forces acting on each atom. A second difficulty is associated with time scales. Since the atoms are vibrating very rapidly indeed, the film frames must be kept very close together if the entire movie is going to be sensible. These snapshots must be on the order of only femtoseconds apart. It thus becomes practically impossible to follow a trajectory that might require seconds to pass from reactants to products; picosecond and nanosecond trajectories are more the rule. The process is further complicated by the fact that atoms are not really balls that respond classically to forces. Rather, their light masses endow them with a quantum behavior that is not easily modeled by Newtonian physics.

As an example, a recent molecular dynamics calculation attempted to study the transfer of a proton between OH^- groups in the context of aqueous solvent [70]. The $HOH{\cdot\cdot}OH^-$ system was restrained in the sense that the interoxygen distance was held fixed (to 2.9 Å), and the bridging proton was constrained to the $OH{\cdot\cdot}O$ axis. This H-bond length leads to a sizable proton transfer barrier, much larger than would occur in the shorter $R(O{\cdot\cdot}O)$ if the system was left to vibrate freely. Solvent was incorporated by surrounding the central $HOH{\cdot\cdot}OH^-$ by 216 water molecules.

The trajectory was followed over a period of 6 ps. During that time period, the bridging proton typically oscillated back and forth within one of the two wells in the proton transfer potential. On average, every 300 fs or so, the proton was found to hop across to the other well, and remain there for a same period of time until hopping back to the original well. The solvent molecules were found to respond rapidly to the proton's change of position. That is, the $HOH{\cdot\cdot}OH^-$ configuration is stabilized by an arrangement of waters that act as proton donors in H-bonds to the righthand group with the negative charge. Upon hopping of the central proton to form the $^-HO{\cdot\cdot}HOH$ geometry, the waters rearrange themselves so as to form H-bonds with the group on the left. These results support the general notion that the proton transfer can be 'catalyzed' by solvent fluctuations which might preferentially stabilize the motion of the proton [71–74].

Like the theoretical methods discussed above, molecular dynamics can also be applied to a larger biological system. To focus on one particular recent example, Merz's group considered the proton transfer mechanism of human carbonic anhydrase II, considering it in its fully hydrated form [75]. Of particular interest was the nature of the bridge of water molecules extending between the zinc atom and an important histidine residue [76–78]. The atoms of the enzyme and more than 10 000 surrounding waters moved within the context of an all-atom force field, with the groups directly involved in the proton transfer treated by a quantum mechanical calculation.

Time steps of 1.5 fs were taken to generate the trajectories, that encompassed as long as 1 ns.

The simulations indicated that the pertinent H-bond network remains largely intact throughout the simulation, particularly for one particular configuration involving zinc and a neutral water molecule. Their simulations suggested that a bridge containing three water molecules was most common, although there were periods when it contained anywhere between two and six such molecules. The experimental dynamics of the proton shuttle process were explained to be consistent with the duration of bridges that can span the two groups involved, usually less than about 100 ps, but some as short as 1 ps. This group suggested that the rate of proton shuttling is controlled by the transfer of the first proton from the zinc-bound water to the first bridging molecule to form a zinc-bound hydroxide plus hydronium. As a consequence, any deuterium isotope effects that might be detected in this system are probably due to one particular proton transfer between the water bound to the zinc and the first water molecule in the bridge.

References

[1] R.D. Gandour and R.L. Schowen, Transition States of Biochemical Processes, Plenum, New York, 1978.
[2] R.P. Bell, The Tunnel Effect in Chemistry, Chapman and Hall, London, 1980.
[3] L. Melander and W.H. Saunders, Reaction Rates of Isotopic Molecules, Krieger, Malabar, FL, 1987.
[4] I.N. Levine, Quantum Chemistry, Prentice-Hall, Englewood Cliffs, NJ, 1991.
[5] S. Scheiner, M. Cuma, J. Am. Chem. Soc. 118 (1996) 1511–1521.
[6] A. Engdahl, B. Nelander, J. Chem. Phys. 86 (1987) 1819–1823.
[7] M. Cuma, S. Scheiner, J. Phys. Org. Chem. 10 (1997) 383–395.
[8] L.A. Curtiss, J.A. Pople, J. Mol. Spectrosc. 61 (1976) 1–10.
[9] S.A.C. McDowell, A.D. Buckingham, Chem. Phys. Lett. 182 (1991) 551–555.
[10] M.D. Schuder, D.J. Nesbitt, J. Chem. Phys. 100 (1994) 7250–7267.
[11] B. Nelander, L. Nord, J. Phys. Chem. 86 (1982) 4375–4379.
[12] A. Engdahl, B. Nelander, J. Chem. Phys. 91 (1989) 6604–6612.
[13] B. Nelander, J. Chem. Phys. 72 (1980) 77–84.
[14] A. Engdahl, B. Nelander, J. Phys. Chem. 90 (1986) 4982–4987.
[15] D.A. Weil, D.A. Dixon, J. Am. Chem. Soc. 107 (1985) 6859–6865.
[16] J.W. Larson, T.B. McMahon, J. Phys. Chem. 91 (1987) 554–557.
[17] S.T. Graul, M.D. Brickhouse, R.R. Squires, J. Am. Chem. Soc. 112 (1990) 631–639.
[18] A.E. Edison, J.L. Markley, F. Weinhold, J. Phys. Chem. 99 (1995) 8013–8016.
[19] I.W.M. Smith, Kinetics and Dynamics of Elementary Gas Reactions, Butterworth, London, 1980.
[20] H. Eyring, S.H. Lin and S.M. Lin, Basic Chemical Kinetics, Wiley, New York, 1980.
[21] K.J. Laidler, Chemical Kinetics, Harper and Row, Cambridge, 1987.
[22] E. Wigner, Phys. Chem. B19 (1932) 203.
[23] M.F. Bigeleisen, M. Goepert-Mayer, J. Chem. Phys. 15 (1947) 261–267.
[24] W.L. Hase, Acc. Chem. Res. 16 (1983) 258–264.
[25] P.J. Robinson and K.A. Holbrook, Unimolecular Reactions, Wiley-Interscience, New York, 1972.
[26] W. Forst, Theory of Unimolecular Reactions, Academic, New York, 1973.
[27] W.H. Miller, J. Am. Chem. Soc. 101 (1979) 6810–6814.
[28] S. Scheiner, J. Am. Chem. Soc. 103 (1981) 315–320.
[29] T. Kar, S. Scheiner, J. Am. Chem. Soc. 117 (1995) 1344–1351.
[30] S. Scheiner, Acc. Chem. Res. 27 (1994) 402–408.
[31] X. Duan, S. Scheiner, J. Am. Chem. Soc. 114 (1992) 5849–5856.
[32] S. Scheiner, J. Mol. Struct. 321 (1994) 1–10.
[33] S. Scheiner, Z. Latajka, J. Phys. Chem. 91 (1987) 724–730.
[34] G. Brunton, D. Griller, L.R.C. Barclay, K.U. Ingold, J. Am. Chem. Soc. 98 (1976) 6803–6811.
[35] G. Brunton, J.A. Gray, D. Griller, L.R.C. Barclay, K.U. Ingold, J. Am. Chem. Soc. 100 (1978) 4197–4200.
[36] K.-H. Grellman, H. Weller, E. Tauer, Chem. Phys. Lett. 95 (1983) 195–199.
[37] K.-H. Grellman, U. Schmitt, H. Weller, Chem. Phys. Lett. 88 (1982) 40–45.
[38] K. Tokumura, Y. Watanabe, M. Itoh, J. Phys. Chem. 90 (1986) 2362–2366.
[39] A. Bromberg, K.A. Muszkat, E. Fischer, F.S. Klein, J. Chem. Soc. Perkin Trans. II (1972) 588–591.
[40] A. Campion, F. Williams, J. Am. Chem. Soc. 94 (1972) 7633–7637.
[41] O.D. Yakimchenko, Y.S. Lebedev, Int. J. Radiat. Phys. Chem. 3 (1971) 17.
[42] A.M. Mebel, L.V. Moskaleva, M.C. Lin, J. Mol. Struct. (Theochem) 461 (1999) 223–238.
[43] M. Demissy, R. Lesclaux, J. Am. Chem. Soc. 102 (1980) 2897–2902.
[44] W. Hack, P. Rouveirolles, H.G. Wagner, J. Phys. Chem. 90 (1986) 2505–2511.

[45] J.W. Sutherland, J.V. Michael, J. Chem. Phys. 88 (1988) 830–834.
[46] J. Ehbrecht, W. Hack, P. Rouveirolles, H.G. Wagner, Ber. Bunsenges. Phys. Chem. 91 (1987) 700–708.
[47] G. Hennig, H.G. Wagner, Ber. Bunsenges. Phys. Chem. 99 (1995) 863–869.
[48] J. Rucker, J.P. Klinman, J. Am. Chem. Soc. 121 (1999) 1997–2006.
[49] J. Bigeleisen, J. Chem. Phys. 17 (1949) 675–678.
[50] F. Jensen, S.S. Glad, J. Am. Chem. Soc. 116 (1994) 9302–9310.
[51] W.P. Huskey, R.L. Schowen, J. Am. Chem. Soc. 105 (1983) 5704–5706.
[52] Y. Cha, C.J. Murray, J.P. Klinman, Science 243 (1989) 1325.
[53] T. Jonsson, D.E. Edmondson, J.P. Klinman, Biochemistry 33 (1994) 14871–14878.
[54] A. Kohen, T. Jonsson, J.P. Klinman, Biochemistry 36 (1997) 2603–2611.
[55] Y. Kim, D.G. Truhlar, M.M. Kreevoy, J. Am. Chem. Soc. 113 (1991) 7837–7847.
[56] J. Basran, M.J. Sutcliffe, N.S. Scrutton, Biochemistry 38 (1999) 3218–3222.
[57] R.A. Marcus, N. Sutin, Biochim. Biophys. Acta 811 (1985) 265–322.
[58] A.D. Isaacson, L. Wang, S. Scheiner, J. Phys. Chem. 97 (1993) 1765–1769.
[59] D.G. Truhlar, A. Kuppermann, J. Am. Chem. Soc. 93 (1975) 1840–1851.
[60] K. Fukui, S. Kato, H. Fujimoto, J. Am. Chem. Soc. 97 (1975) 1–7.
[61] A.D. Isaacson, D.G. Truhlar, J. Chem. Phys. 76 (1982) 1380–1391.
[62] B.C. Garrett, D.G. Truhlar, J. Phys. Chem. 83 (1979) 1079–1112.
[63] D.G. Truhlar, A.D. Isaacson, R.T. Skodje, B.C. Garrett, J. Phys. Chem. 86 (1982) 2252–2261.
[64] R.T. Skodje, D.G. Truhlar, B.C. Garrett, J. Chem. Phys. 77 (1982) 5955–5976.
[65] L. Masgrau, A. Gonz‡lez-Lafont, J.M. Lluch, J. Phys. Chem. A 103 (1999) 1044–1053.
[66] C. Alhambra, J. Gao, J.C. Corchado, J. Villö, D.G. Truhlar, J. Am. Chem. Soc. 121 (1999) 2253–2258.
[67] S.R. Anderson, V.E. Anderson, J.R. Knowles, Biochemistry 33 (1994) 10545–10555.
[68] Y.-P. Liu, D.-H. Lu, A. Gonz‡lez-Lafont, D.G. Truhlar, B.C. Garrett, J. Am. Chem. Soc. 115 (1993) 7806–7817.
[69] J. Bigeleisen, J. Chem. Phys. 23 (1955) 2264–2267.
[70] I. Tuñón, M.T.C. Martins-Costa, C. Millot, M.F. Ruiz-López, J. Chem. Phys. 106 (1997) 3633–3642.
[71] D. Borgis, G. Tarjus, H. Azzouz, J. Chem. Phys. 97 (1992) 1390–1400.
[72] F.R. Tortonda, J.-L. Pascual-Ahuir, E. Silla, I. Tuñón, J. Phys. Chem. 97 (1993) 11087–11091.
[73] B.E. Conway, J.O. Bockris, H. Linton, J. Chem. Phys. 24 (1956) 834–850.
[74] J.L. Kurz, L.C. Kurz, J. Am. Chem. Soc. 94 (1972) 4451–4461.
[75] S. Toba, G. Colombo, K.M. Merz, J. Am. Chem. Soc. 121 (1999) 2290–2302.
[76] C. Tu, D.N. Silverman, C. Forsman, B.-H. Honsson, S. Lindskog, Biochemistry 28 (1989) 7913–7918.
[77] K. HŒkansson, M. Carlsson, L.A. Svensson, A. Liljas, J. Mol. Biol. 227 (1992) 1192–1204.
[78] D. Lu, G.A. Voth, J. Am. Chem. Soc. 120 (1998) 4006–4014.